IEEE Access
Multidisciplinary | Rapid Review | Open Access Journal

Received 4 September 2022, accepted 11 September 2022, date of publication 16 September 2022,
date of current version 26 September 2022.

Digital Object Identifier 10.1109/ACCESS.2022.3207153

RESEARCH ARTICLE

Military Vehicle Object Detection Based on Hierarchical Feature Representation and Refined Localization

YAN OUYANG, XINQING WANG, RUIZHE HU, HONGHUI XU, AND FAMING SHAO
Department of Mechanical Engineering, College of Field Engineering, Army Engineering University, Nanjing 210007, China

Corresponding author: Xinqing Wang (wangxinqing510@163.com)

This work was supported in part by the China National Key Research and Development under Program 2016YFC0802904, in part by the National Natural Science Foundation of China under Grant 61671470, and in part by the 62nd Batch of Funded Projects of China Postdoctoral Science Foundation under Grant 2017M623423.

ABSTRACT Military vehicle object detection technology in complex environments is the basis for the implementation of reconnaissance and tracking tasks for weapons and equipment, and is of great significance for information and intelligent combat. In response to the poor performance of traditional detection algorithms in military vehicle detection, we propose a military vehicle detection method based on hierarchical feature representation and reinforcement learning refinement localization, referred to as MVODM. First, for the military vehicle detection task, we construct a reliable dataset MVD. Second, we design two strategies, hierarchical feature representation and reinforcement learning-based refinement localization, to improve the detector. The hierarchical feature representation strategy can help the detector select the feature representation layer suitable for the object scale, and the reinforcement learning-based refinement localization strategy can improve the accuracy of the object localization boxes. The combination of these two strategies can effectively improve the performance of the detector. Finally, the experimental results on the homemade dataset show that our proposed MVODM has excellent detection performance and can better accomplish the detection task of military vehicles.

INDEX TERMS Military vehicle objects, object detection, reinforcement learning, hierarchical feature representation.

NOMENCLATURE

MVD	Military vehicle dataset.
B_t	Bounding box information for time step t.
$\theta_t(i)$	Vector of feature representations of military vehicle instance i at time step t.
k_t	The final concise description of instance i at time step t.
s_t	The state representation of the agent at time step t.
a_t	The action performed by the agent at time step t.
$r_1(s_t, s_{t+1})$	Reward for agent transfer from state s_t selection action a_t to state s_{t+1}.
$r_2(T)$	The sequence reward that the agent receives at the end of the action sequence.

The associate editor coordinating the review of this manuscript and approving it for publication was Zhongyi Guo.

I. INTRODUCTION

With the development and progress of technology, modern warfare is gradually moving into the era of informationization and intelligence. In the future information-based warfare, efficient battlefield situational awareness capability is undoubtedly the key to guarantee the victory of war, and the military powers are now actively strengthening the research of related technology in this aspect [1]. Battlefield situational awareness includes several tasks such as reconnaissance, surveillance, intelligence, damage assessment, beacon

indication, and information resource management and control. Among these tasks, the identification and localization of military targets is a basic and critical technology [2]. Therefore, research on automatic detection technology for military targets in complex battlefield environments is of great significance to improve battlefield situational awareness.

In recent years, with the boom of deep learning, deep learning has been widely used in medical diagnosis [3], smart cities [4] and intelligent robots [5]. In object detection, the introduction of deep learning has greatly improved the detection performance, and deep learning-based object detection techniques have gradually replaced the traditional manual feature-based methods. After continuous research and improvement by scholars, the current mainstream object detection methods have made significant progress in the detection of common targets. However, for military targets, due to their secrecy and environmental complexity, there are often greater difficulties for the detection of military targets [6]. In order to further improve the battlefield situational awareness, this paper addresses the detection of vehicle targets in military targets, aiming to improve the detection performance of military vehicle targets.

The following difficulties exist in military vehicle object detection: first, military vehicle targets lack corresponding datasets for detection model training due to their secrecy, second, military vehicles are located in complex environments and detection is susceptible to background interference, and finally, military vehicle targets have a wide scale distribution and large scale variation, especially some of them present extremely small sizes due to the long acquisition distance. In recent years, the combination of reinforcement learning and deep learning has yielded significant results in solving intelligent decision-making and optimization problems. [7] proposed a game-based deep reinforcement learning method, which is effective in optimizing the energy consumption problem of MEC systems. [8] proposed a recurrent deep reinforcement learning method for solving the control problem of spectrum access in wireless networks. Based on the inspiration from the above studies, we consider introducing reinforcement learning into our research. Specifically, in order to solve the difficulties in military vehicle object detection, we propose a military vehicle object detection method based on hierarchical feature representation and reinforcement learning refinement localization. Our main efforts are summarized as follows.

(1) To address the lack of military vehicle target datasets, we downloaded images and videos from the Internet and performed a series of processing on them to finally construct a military vehicle dataset (MVD) that meets our research needs;

(2) To address the multi-scale problem in military vehicle detection, we propose a hierarchical feature representation strategy, which can help objects of different scales to select the most appropriate representation feature layer and thus improve the detection performance;

(3) To address the problem of inaccurate object localization in the original detection method, we design a refined localization strategy based on reinforcement learning, which can effectively improve the localization accuracy of the prediction frame and enhance the detector performance;

(4) The experimental results on the self-built dataset show that our proposed MVODM has excellent detection performance and is able to perform the detection task of military vehicles better.

The remainder of this paper is organized as follows: we briefly review related work on military target detection in Section 2. Section 3 presents the military vehicle dataset we constructed. In Section 4, we present our MVODM in detail. In Section 5, we conduct extensive experiments and analyze and discuss the experimental results. Finally, Section 6 summarizes the full work.

II. RELATED WORK

A. GENERAL OBJECT DETECTION

The task of object detection is to automatically identify and locate the object to be detected from an image or video. It has been a hot research topic in the field of computer vision. Traditional object detection methods mainly use hand-designed features to train classifiers, which include HOG [9], Haar [10], CSS [11], LBP [12], and ICF [13]. However, in recent years, with the development of convolutional neural networks (CNNs) [14], object detection methods based on deep learning [15] have gradually attracted the attention and research of a wide range of scholars. The current mainstream deep learning-based object detection models can be divided into two main categories: proposal-based two-stage detectors and proposal-free one-stage detectors. The R-CNN series [16], [17], [18] is representative of two-stage detectors. This class of detectors first generates several proposals of regions of interest that may contain targets in the first stage, and then uses classifiers and border regression to detect targets on the proposed regions in the second stage. In contrast, one-stage detectors, such as the YOLO series [19], [20], [21], [22] and SSD [23], do not need to generate region of interest proposals and can directly classify and localize targets. In general, one-stage target detectors are much faster than two-stage target detectors, but the detection accuracy is relatively poor, which is determined by their structure.

B. MILITARY OBJECT DETECTION

The introduction of deep learning-based object detection methods into the military field can effectively improve battlefield situational awareness. In recent years, scholars in related fields have also gradually carried out research on military object detection based on deep learning methods. In the framework of Faster R-CNN, [24] designed a top-down agglomerative network to detect military armored targets. Reference [25] used Faster R-CNN and image pyramids to solve the armor target detection problem. Reference [26] proposed a military object detection framework based on Gabor convolutional kernel and deep feature pyramid network, which achieved better detection results. By using

FIGURE 1. Example of a partial sample of the military vehicle dataset.

three-channel images fusing temporal, spatial and thermal information to detect military targets and fine-tuning them using transfer learning methods, [27] was able to perform the military target detection task better. Reference [28] proposed a deep transfer learning technique in order to solve the problem of military target recognition under few-shot conditions. Reference [29] proposed a multi-level capsule network to improve military target detection accuracy. Reference [30] studied the work related to the deployment of mainstream algorithms on UAVs for military target detection, and laid the foundation for the application of the algorithms.

III. HOMEMADE MILITARY VEHICLE DATASET

Datasets are one of the most important parts of object detection work. Currently, publicly available datasets for generic and vehicle target detection tasks, such as COCO [31] and KITTI [32], are relatively well established and can meet the needs of detection tasks. However, none of these datasets involve military vehicle targets in complex battlefield environments and cannot be directly used for the detection of military vehicles. In previous research work on military object detection, scholars have constructed their own datasets in response to the lack of military target datasets [26], [29], [30]. However, these datasets also generally have some problems: (1) firstly, scholars' homemade datasets are seldom publicly available and cannot be directly used, (2) secondly, these datasets usually do not consider the scale of military targets and are not well targeted for realistic military target detection tasks, (3) finally, these datasets contain a wide range of military targets that are usually different from the military vehicle detection task of this paper. Therefore, a new military vehicle dataset (MVD) was constructed to better carry out the research work in this paper.

A. CAPACITY OF MVD

We obtain images containing military vehicles by two means: (1) downloading the desired military vehicle images directly from the Internet and filtering them, discarding unreasonable images, and (2) sampling frames of publicly available military video materials (e.g., military exercises and training) to obtain military vehicle images, again making a reasonable selection of the images obtained. A total of five typical

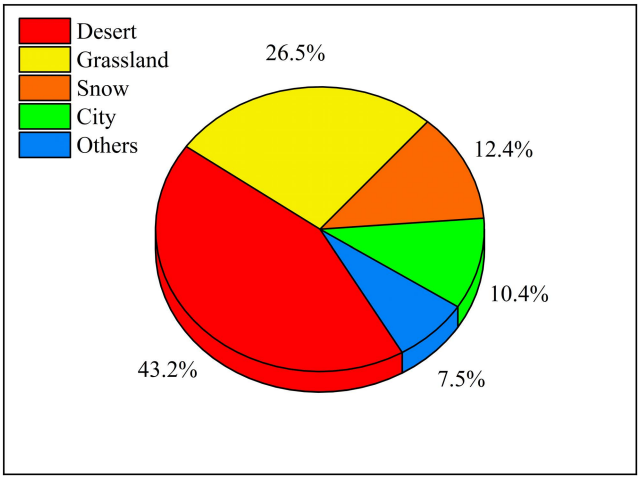

FIGURE 2. Proportional distribution of military vehicle targets for different scenarios.

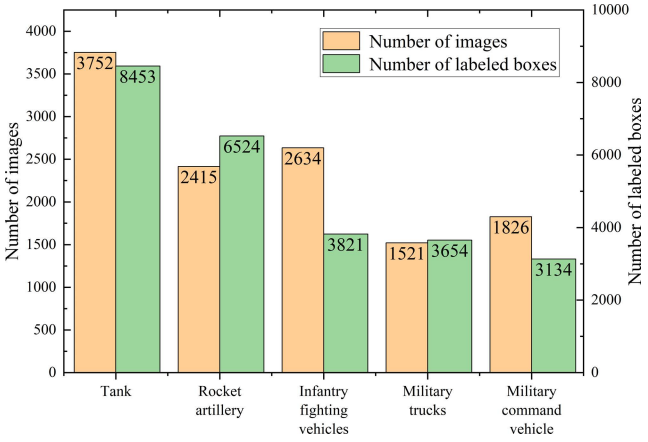

FIGURE 3. Statistics on the number of different military targets in the dataset, including the number of images and the number of labeled boxes.

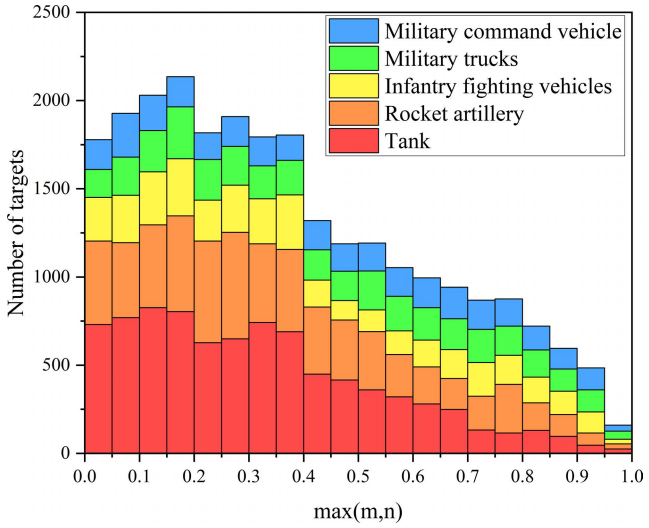

FIGURE 4. Scale distribution of military vehicle targets, with m and n representing the ratio of the width and height of the target to the width and height of the image, respectively.

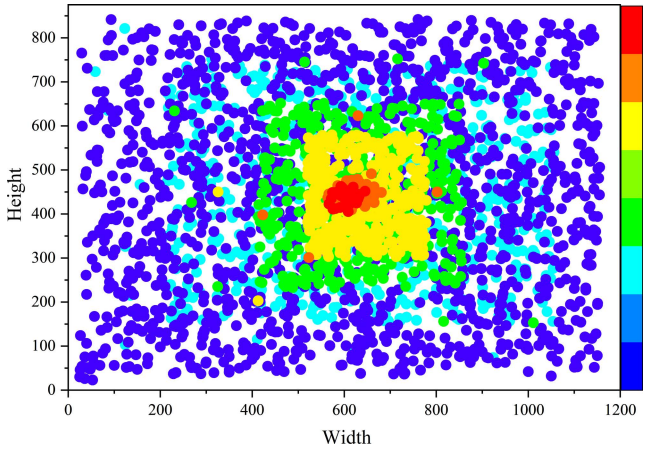

FIGURE 5. Location distribution of military vehicle targets.

military vehicle targets are included in the MVD constructed in this paper: tank, rocket artillery, infantry fighting vehicles, military trucks, and military command vehicle. These military vehicles come from a variety of complex battlefield environments, such as desert, grassland, snow, and cities. In Figure 1, we show some sample examples from our MVD, column 1 shows a single small-scale target example, columns 2 and 3 show multiple target examples in different environments, and column 4 shows a large-scale target example. As can be seen from the Figure 1, our MVD contains various possible scenarios for military vehicle targets, such as city in row 1, column 2, grassland in row 2, column 1 and snow in row 3, column 2, and in Figure 2, we count the number of military vehicle targets contained in different scenes. Our MVD contains a total of 12,148 military vehicle images, and we uniformly convert the collected images to.JPG format of 1200×875 size and number all images uniformly. Then we used LabelImg software to label the military vehicle targets in the images and obtained a total of 25586 valid labeled boxes. We randomly selected 70% of the images from different types of military vehicle targets as the training set samples and the remaining 30% as the test set samples. Figure 3 shows the image and annotation frame statistics of various types of military vehicle targets.

B. SCALE AND POSITION OF MVD

We also performed statistics on the scale information and location information of the military vehicle targets in our MVD. The statistical results are shown in Figure 4 and Figure 5, respectively. We calculate the ratio of the width of the military vehicle target to the width of the image, m, and the ratio of the height of the military vehicle target to the height of the image, n, and take the larger of m and n to count and evaluate the scale distribution of the MVD. It is clear from Figure 4 that our MVD contains more small-scale targets, which is consistent with the situation in real reconnaissance missions, i.e., small-scale targets are more common. The

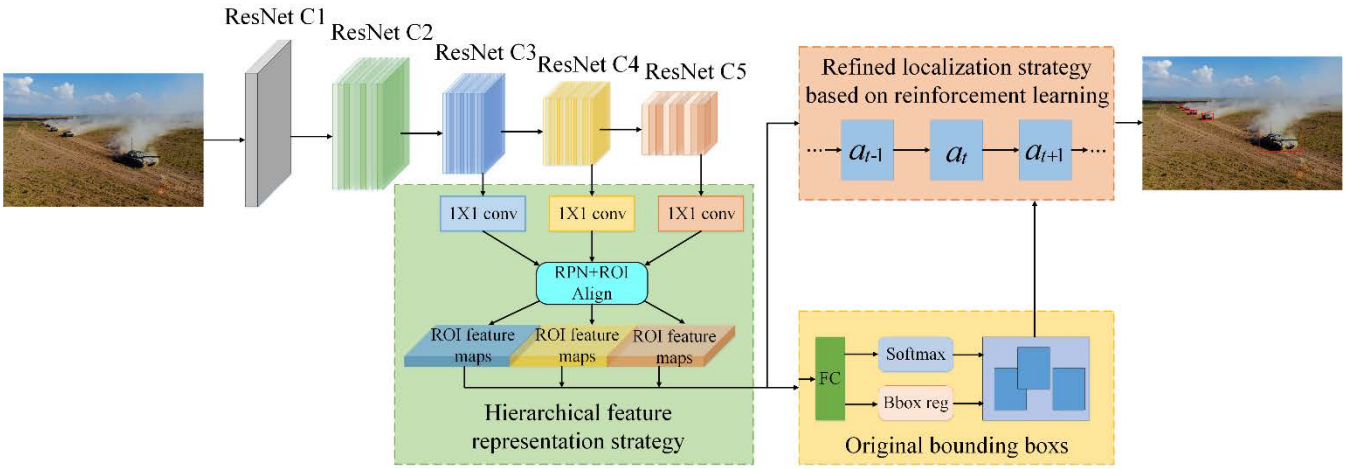

FIGURE 6. The overall framework of Our proposed military vehicle object detection method.

location statistics in Figure 5 show that the military vehicle targets in our dataset are uniformly distributed throughout the image, and this distribution is beneficial for enhancing the robustness of the object detector to location.

IV. OUR APPROACH

In this section, we describe the specific implementation of our proposed military vehicle object detection method (MVODM). MVODM is divided into two main phases: the first phase is mainly used to generate a hierarchical feature representation of the region of interest and the original bounding box, and the second phase uses reinforcement learning strategies to select the most appropriate feature representation layer and refine the localization of the target to be detected. The overall framework of our proposed method is shown in Figure 6. First, the input image is fed into the backbone network to perform feature extraction, and in this paper, we use ResNet50 as the feature extraction network. Then, the extracted features perform a hierarchical feature representation strategy and are fed into the subsequent network to generate the initial bounding box. Finally, the hierarchical features and the initial bounding box are fed together into the reinforcement learning-based refinement localization module to obtain the final detection results.

A. HIERARCHICAL FEATURE REPRESENTATION STRATEGY

Generally speaking, the high level feature extraction layer tends to capture the global overall information of the image and the semantic information of the target, which can provide robustness support for appearance changes. However, due to the reduced spatial resolution, the high level feature extraction layer has limitations in target localization accuracy, especially when facing small scale targets. However, low level feature extraction layers are able to capture more accurate localization information, but lack robustness to target changes. Meanwhile, previous studies [33] have shown that high level feature maps have better activation for large scale objects, while small scale objects respond strongly in low level feature maps. Therefore, to address the multi-scale problem in our military vehicle detection task, we consider using a hierarchical feature representation strategy to generate different levels of feature representations of the object to be detected and select the best feature representation by a subsequent reinforcement learning strategy to improve the detection performance. Specifically, as shown in the green box in Figure 6, we selected C_3, C_4 and C_5 from ResNet50 to serve as the workspace for the layered feature representation. We perform a 1×1 convolution operation on the output of these three feature layers and feed RPN and ROI Align to obtain the feature vectors of military vehicle target proposals for each layer, which are fed into a fully connected layer for generating initial military vehicle bounding box predictions, including softmax classification and bounding box regression.

B. REFINED LOCALIZATION STRATEGY BASED ON REINFORCEMENT LEARNING

To more accurately localize military vehicle targets in images, we consider introducing reinforcement learning to further refine the target bounding box. Meanwhile, inspired by previous work [34], we use a recurrent neural network-based framework to design our refinement localization strategy. Figure 7 illustrates part of the recurrent process of our refinement localization strategy.

As shown in Figure 7, at each time step t, B_{t-1} represents the bounding box information of the previous time step (when t=1, B_0 is the original bounding box information), and $\theta_t(i)$ represents the feature representation vector of military vehicle instance i at time step t. It should be noted that the size of $\theta_t(i)$ varies depending on the selected feature layer because we use a hierarchical feature representation strategy. In this paper, the number of output feature map channels for C_3, C_4 and C_5 are 512, 1024, and 2048, respectively. By implementing ROI Align (divided into 2×2) for the region of interest

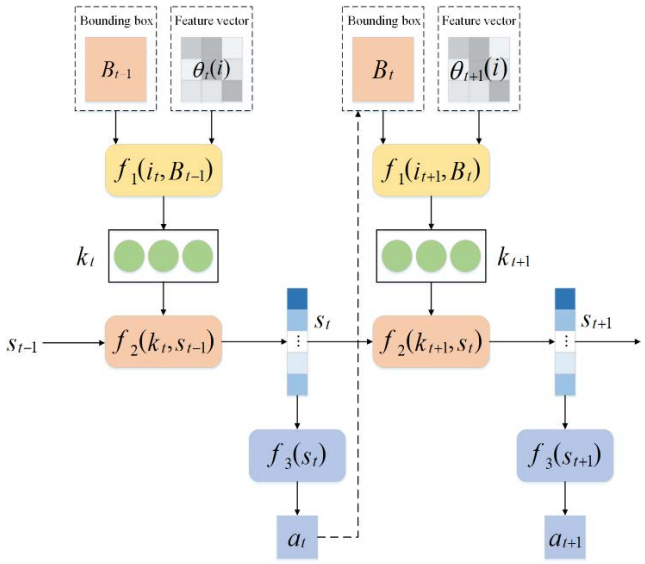

FIGURE 7. The specific implementation process of the reinforcement learning-based refinement localization strategy.

in the corresponding layer, the final dimension of the feature representation vectors for the three different feature layers are 2048 ($2 \times 2 \times 512$), 4096 and 8192, respectively. The final concise description of instance i at layer j is then obtained by a fully connected layer and the ReLU activation function [34]:

$$k_t = f_1(i_t, B_{t-1}) = \sigma(w_1^j \theta_t(i)) \tag{1}$$

where $\sigma(\cdot)$ represents the ReLU activation function, j denotes the feature layer selected at time t, $j \in \{3, 4, 5\}$,and w_1^j represents the weight parameter of the fully connected layer. Empirically, we set the dimension of k_t to 1024. Meanwhile, we combine the past state information s_{t-1} to generate the new state s_t:

$$s_t = f_2(k_t, s_{t-1}) = \psi(w_2^1 k_t + w_2^2 s_{t-1}) \tag{2}$$

where $\psi(\cdot)$ denotes the Tanh activation function, and w_2^1 and w_2^2 represent the weight parameters of k_t and s_{t-1}, respectively. In this paper, the dimension of s_t is set to 64. Finally, we perform the coordinate transformation of the bounding box by randomly selecting the execution action a_t conditional on the current state as follows

$$a_t = f_3(s_t) = \varepsilon(w_3 s_t) \tag{3}$$

where $\varepsilon(\cdot)$ denotes the Softmax function and w_3 represents the weight parameter. a_t is a 10-dimensional vector corresponding to the 10 different transformation actions in our action set.

Next, we instantiate each element of the Markov Decision Process (MDP) [35] in reinforcement learning. These elements include state S, action A, and reward function R. At each time step t,agent observes the environment state $s_t \in S$, selects an action $a_t \in A$ based on the given policy, and then moves to the next state s_{t+1}, in which the agent will

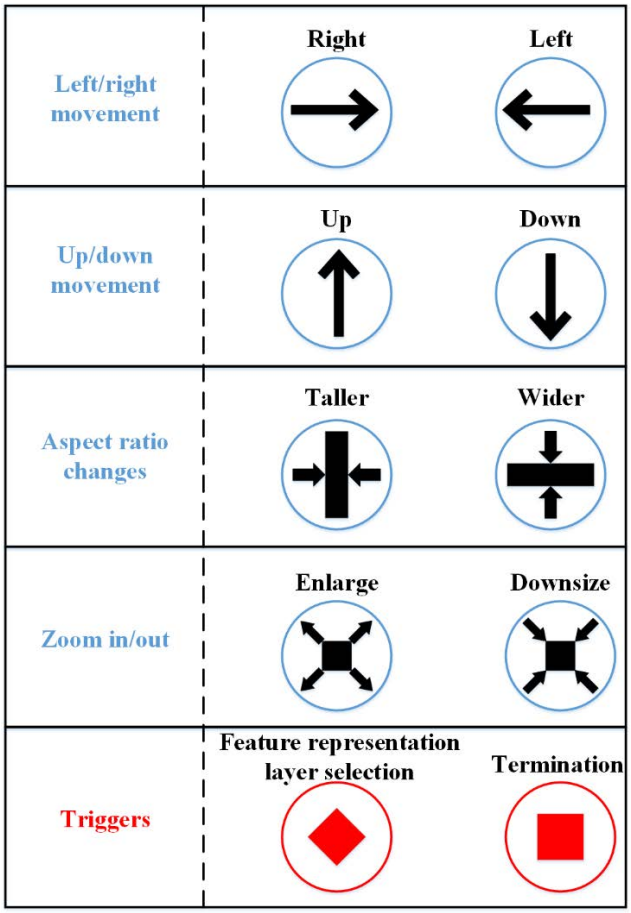

FIGURE 8. Action ensemble A used in the reinforcement learning-based refinement localization strategy.

receive a reward $r_t \in R$ from the environment feedback. It is important to note that agent receives rewards for each decision (i.e., selected action) only during training, while in testing, we follow the trained model strategy and agent does not receive rewards.

(1) **State:** As previously described, the state s_t at time step t is a 64-dimensional vector containing the historical state information, the current bounding box information, and the selected corresponding layer feature representation. s_t is calculated by Equation (2).

(2) **Action:** As shown in Figure 8, we designed a total of 10 different types of actions in action set A. These actions include 8 actions for coordinate transformation and 2 actions for triggering. These actions include 8 actions for coordinate transformation and 2 trigger actions. Considering all possible situations during the coordinate conversion, the coordinate conversion actions are subdivided into four types: left-right movement, up-down movement, aspect ratio change, and zoom-in/out. The trigger action is mainly used to select the best feature representation layer at the beginning of the action sequence and to terminate the coordinate transformation at the end of the action sequence.

In this paper, we define the bounding box information as $B_t = (b_t^x, b_t^y, b_t^w, b_t^h)$, where (b_t^x, b_t^y) represents the coordinates of the upper left corner of the bounding box, and b_t^w and b_t^h represent the width and height of the bounding box, respectively. For the four types of transformation actions, the specific coordinate transformation is calculated as:

1) shifts left and right: $b_{t+1}^x = b_t^x + c, c \in R$, to the right when c is positive and to the left when c is negative.
2) shifting up and down: $b_{t+1}^y = b_t^y + c, c \in R$, shifting down when c is positive and up when c is negative.
3) aspect ratio change: $b_{t+1}^h = b_t^h + c, c \in R$ is used to change the height and $b_{t+1}^w = b_t^w + c, c \in R$ is used to change the width.
4) Zoom in and out: $b_{t+1}^h = b_t^h \times c, b_{t+1}^w = b_t^w \times c$,when c∈(0,1) is zoomed out, when c>1 is zoomed in.

(3) **Reward function** The reward function consists of two parts: action reward and sequence reward. For the action reward, we design the reward function by calculating the difference between the Intersection-over-Union (IoU) of the bounding box (B) and the ground truth box (G) before and after the coordinate transformation [36]. Specifically, the reward for transferring from state s_t to state s_{t+1} by selecting action a_t is:

$$r_1(s_t, s_{t+1}) = \begin{cases} 1, & \text{IoU}(B_{t+1}, G_{t+1}) - \text{IoU}(B_t, G_t) > 0 \\ 0, & \text{IoU}(B_{t+1}, G_{t+1}) - \text{IoU}(B_t, G_t) = 0 \\ -1, & \text{IoU}(B_{t+1}, G_{t+1}) - \text{IoU}(B_t, G_t) < 0 \end{cases} \tag{4}$$

At the end of the action sequence, we designed an additional sequence reward to evaluate this sequence:

$$r_2(T) = \begin{cases} 4, & \textit{if } \text{IoU}(B_T, G_T) \geq 0.8 \\ 2, & \textit{if } 0.6 \leq \text{IoU}(B_T, G_T) < 0.8 \\ -5, & \textit{otherwise} \end{cases} \tag{5}$$

For the action reward function, since the difference between the IoU of the bounding box (B) and the ground truth box (G) before and after the coordinate transformation is small, using the difference as the reward directly would not provide the agent with enough clear guidance information. Therefore, we quantified the reward as three real numbers $\{1, 0, -1\}$, which can help the agent to better select the action to improve the bounding box. The sequential reward function is designed mainly to encourage the agent to learn a high-performance object localization strategy.

V. EXPERIMENTS

In this section, the experimental results are presented and analyzed and discussed. Section 5.1 describes the specific experimental setup. Section 5.2 shows the results of the ablation study. Section 5.3 shows the detailed assay results.

A. EXPERIMENTAL SETUP

1) IMPLEMENTATION DETAILS

Our experiments were all performed on a GeForce RTX 3090 GPU. For the hierarchical representation of features, we initialize ResNet50 using the pre-trained weights on ImageNet [37]. For the training of the original bounding box proposal network, we used Adam [38] as the optimizer with an initial learning rate set to 10^{-3} and a 10-fold reduction in the learning rate per 7000 iterations, for a total of 25k iterations. The mini-batch consists of 120 object proposals randomly sampled from one image, where the ratio of positive to negative proposals is 1:3. We mark a proposal as positive if its IoU with one ground truth frame is greater than 0.5, and consider it negative if the IoU of the proposal with any ground truth frame is less than 0.3. Considering our refined localization strategy, we set the initial number of proposals per image to 250 rather than more (e.g., 2000), and previous studies [18], [39] have shown that a larger number of proposals has little benefit for detection. For reinforcement learning training, the initial learning rate was set to 10^{-3} and gradually linearly annealed to 0.

2) EVALUATION METRICS

In this paper, we use a total of four evaluation metrics to evaluate the performance of our proposed MVODM, which are precision (P), recall (R), average precision (AP), and mean average precision (mAP). Let P_T be the number of correctly predicted positive samples, P_F be the number of incorrectly predicted positive samples, N_F be the number of incorrectly predicted negative samples, and N_T be the number of correctly predicted negative samples. Then the expression of precision rate is calculated as:

$$P = \frac{P_T}{P_T + P_F} \tag{6}$$

Similarly, the recall rate can be calculated by the following equation

$$R = \frac{P_T}{P_T + N_F} \tag{7}$$

Average precision is an evaluation metric that synthesizes precision and recall, which reflects the performance of the detection model on each class target, and its value can be obtained by calculating the area under the precision-recall (PR) curve. Mean average precision is the mean of the average precision of all classes of targets, which reflects the performance of the detection model over the entire dataset. Meanwhile, to further evaluate the detection performance of our algorithm for small-scale military vehicle objects, we divide the test set into small-scale (S) subsets, large-scale (L) subsets, and all (A) subsets, and report the performance on these subsets separately. The subsets are divided based on S: $0 < \max(m, n) \leq 0.3$,L: $0.3 < \max(m, n) < 1$,A: $0 < \max(m, n) < 1$.

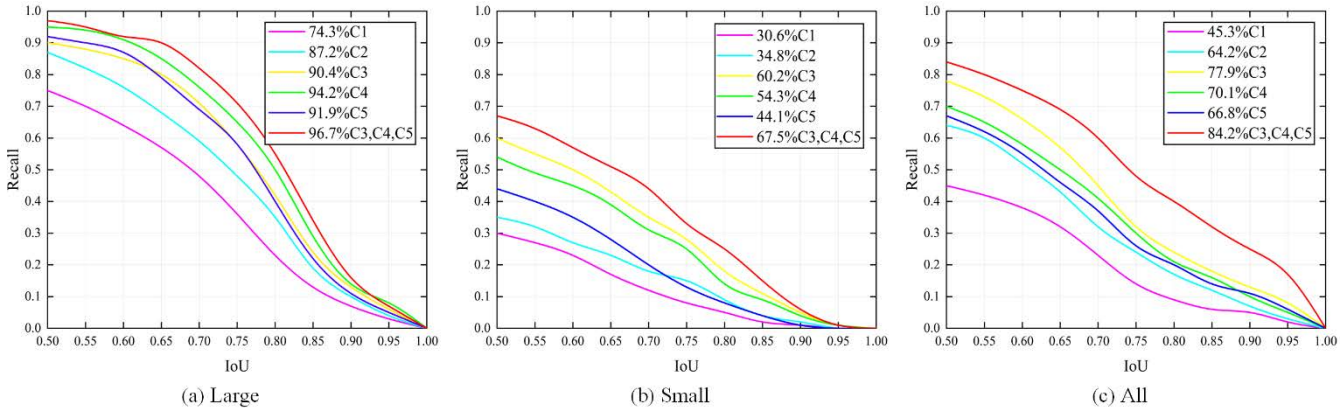

FIGURE 9. Recall-IoU curves on ResNet50 using different feature representation layers alone (C1-C5) and using our layered representation strategy (C3, C4, C5).

TABLE 1. Effectiveness evaluation results of the reinforcement learning-based refinement localization strategy. OPB represents the use of the original proposal box, RLS represents the use of the refinement localization strategy, and the evaluation metric is AP (%).

Method	L	S	A
C3+OPB	70.4	54.1	63.7
C4+OPB	77.6	52.7	70.9
C5+OPB	74.9	51.6	66.2
C3+RLS	78.1	65.2	71.5
C4+RLS	85.4	63.4	78.2
C5+RLS	82.4	62.3	75.8

B. ABLATION STUDIES

We perform ablation experiments to evaluate the effectiveness of two strategies in our MVODM. First, we remove the reinforcement learning-based refinement localization strategy and evaluate the performance of using only the hierarchical feature representation strategy and the original proposal boxes. Then, we evaluate the performance of using the reinforcement learning-based refinement localization strategy directly on different feature layers without the hierarchical feature representation and the original proposal boxes. Finally, we also conduct extended experiments using the reinforcement learning-based refinement localization strategy on the original proposal boxes generated on different feature representation spaces. For all ablation experiments, we report the performance of the method using only the tank target as an example, if not specifically noted.

1) EFFECTIVENESS OF HIERARCHICAL FEATURE REPRESENTATION STRATEGY

We evaluate the effectiveness of our layered feature representation strategy by using different layers of ResNet50 (C1-C5) alone to generate original proposals as the final output and by using the layered representation strategy (C3, C4, C5) to generate original proposals as the final output. In this experiment, we evaluate the performance based on the recall of different IoUs, which are tested on three subsets, and the experimental results are shown in Figure 9. From Figure 9, it is clear that, firstly, C1 and C2 perform less well on all subsets, mainly because the shallower feature layer cannot extract enough feature information and the feature representation is weak. Comparatively, C3 is a good starting point for feature representation. Secondly, we observe that C4 performs best on the large scale subset compared to other individual layers, while C3 shows better performance on the small scale subset, which indicates that the higher feature layer (C4) has better activation for large scale objects, while the lower feature layer (C3) is more suitable for representing small scale objects. Finally, our hierarchical representation strategy achieves optimal performance for either subset. At an IoU threshold of 0.5, our hierarchical representation strategy can achieve 96.7% (L), 67.5% (S), and 84.2% (A) recall, respectively, which is a more significant improvement in detection performance compared to the previous best results for single-layer features by 2.5% (L), 7.3% (S), and 6.3% (A), respectively.

2) EFFECTIVENESS OF REINFORCEMENT LEARNING-BASED REFINEMENT LOCALIZATION STRATEGY

To verify the effectiveness of the reinforcement learning-based refinement localization strategy, we conducted the following experiments: using the refinement localization strategy directly on different feature layers and using the original proposal boxes as the final output on different feature layers. In this experiment, we only evaluate the results on C3-C5 and use the average precision (AP) as the evaluation metric, again, on each of the three subsets. The experimental results are shown in Table 1. Relative to the original proposed box, our refined localization strategy improves the localization results with a larger improvement in AP on all three subsets L, S, and A. Taking C5 as an example, our refined localization strategy is 7.5% (L), 10.7% (S), and 9.6% (A) higher than the original proposal boxes, respectively. Similarly, we note that C4 performs best on the large-size subset, while C3 is superior on the small-scale subset.

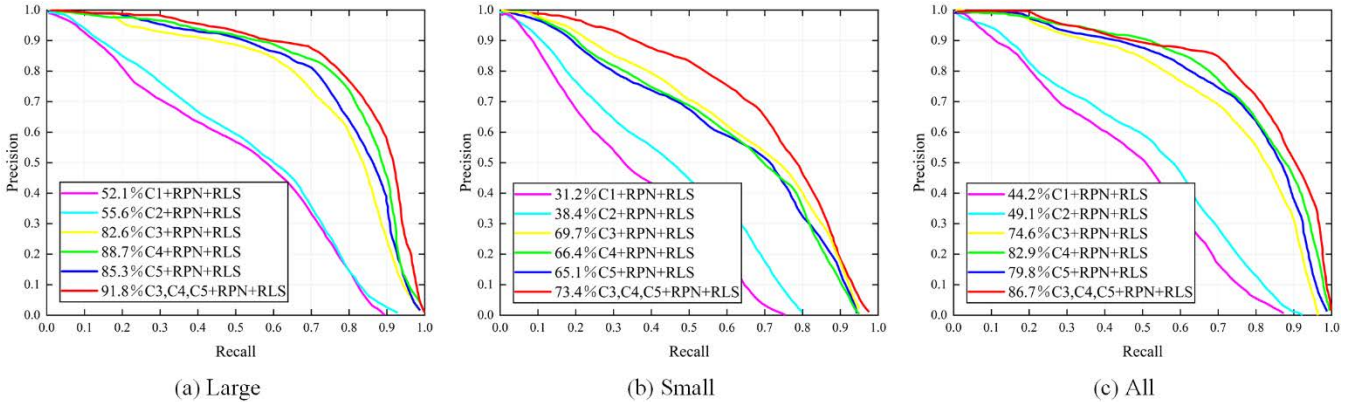

FIGURE 10. Experimental results using the refined localization strategy on the original proposal boxes.

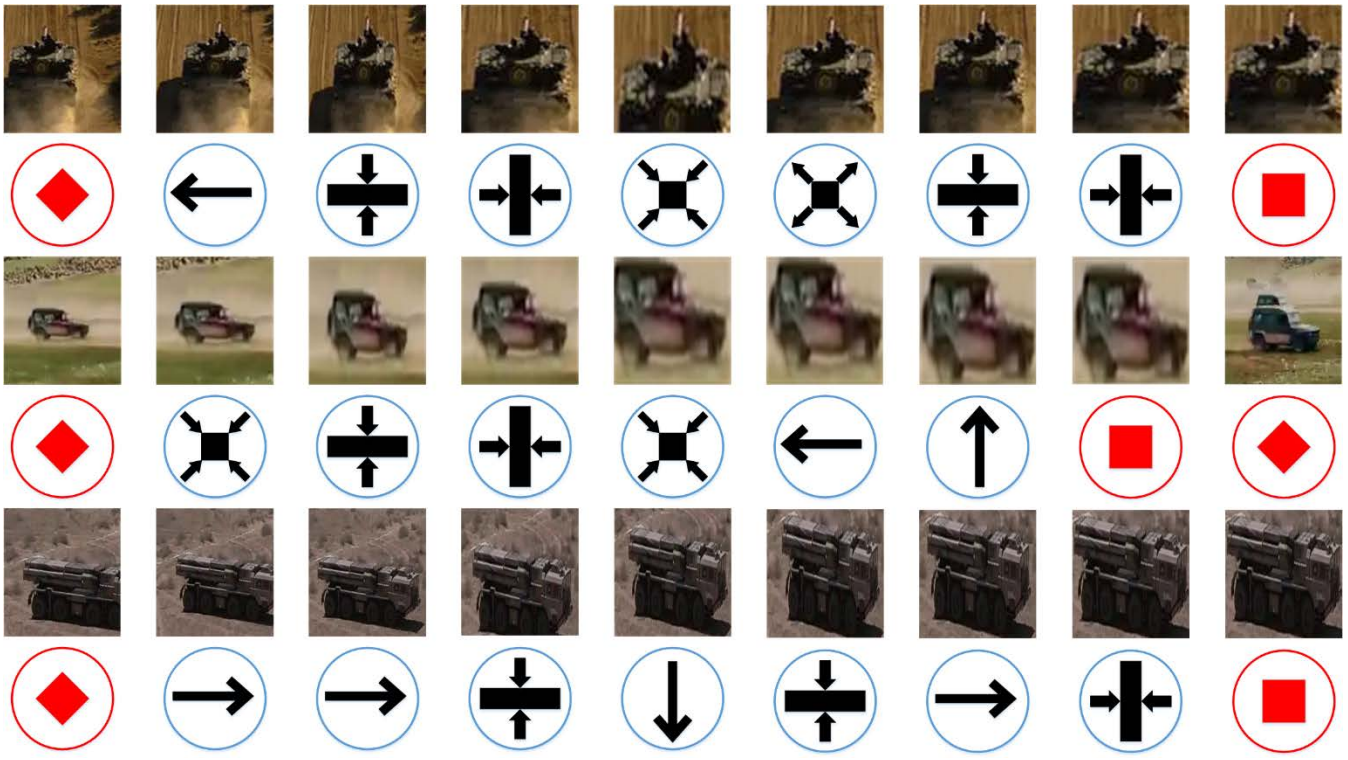

FIGURE 11. Example of the process of refinement localization based on reinforcement learning. (Some images have been resized for aesthetic purposes.)

3) REFINEMENT LOCALIZATION RESULTS ON DIFFERENT FEATURE REPRESENTATION SPACES

To further validate the effectiveness of the combination of our proposed hierarchical feature representation strategy and the refined localization strategy, we conducted extended experiments on different feature representation spaces. Figure 10 shows the PR curves on the three tested subsets. As can be seen from the figure, the performance of combining the two strategies is the best regardless of the subset. On the subsets L, S and A, our proposed method achieves 91.8%, 73.4% and 86.7% AP, respectively. On the one hand, our combined strategy has a clear advantage over other feature representation layers using the original proposal boxes and refinement localization strategies. On the other hand, our combined strategy also achieves significant performance improvement compared to the previous hierarchical representation strategy or refined localization strategy alone.

C. DETECTION RESULTS

1) QUANTITATIVE RESULTS

To validate the effectiveness of our proposed MVODM for detecting military vehicle targets, we compared MVODM with several mainstream object detection algorithms: R-FCN [39], SSD [23], YOLOv3 [21], YOLOv4 [22], and Faster

FIGURE 12. Visual comparison of the detection results of our MVODM and Faster R-CNN. Where green boxes represent correct targets detected, red solid boxes represent false detections, and red dashed boxes represent missed detections.

R-CNN [18]. We trained and tested all the algorithms using our homemade dataset and reported the AP and overall mAP for each class of targets separately, and the experimental results are shown in Table 2. From the data in Table 2, we can see that our proposed MVODM shows excellent performance in detecting military vehicle targets. Specifically, first, for the all subset, our MVODM showed optimal performance for each class of military vehicles, obtaining detection accuracies of 86.7%, 83.2%, 78.4%, 80.9%, and 76.5% for tank, rocket artillery, infantry fighting vehicles, military trucks, and military command vehicle, respectively, exceeding the suboptimal methods by 4.4%, 6.4%, 8.9%, 9.3%, and 8.7%. Second, for the overall object detection performance on different subsets, our MVODM also achieves optimal performance for all of them, achieving 85.6% (L), 66.3% (S) and 81.1% (A) of mAP, respectively. Finally, compared to the baseline detector Faster R-CNN, our MVODM improves the mAP by 7.4% (L), 8.1% (S) and 9.9% (A) on three different subsets, respectively, which strongly validates the effectiveness of our improved strategy.

2) QUALITATIVE RESULTS

First, we show a partial example of action sequences for our proposed reinforcement learning-based refinement localization process in Figure 11. As can be seen, only a limited number of action transformations are required for us to obtain a more appropriate bounding box. Such a bounding box is a further directed (facilitated by rewards) refinement of the original proposed box, which can improve the detection performance to some extent. According to the experimental statistics, about 74% of the objects need less than 10 actions to complete the coordinate transformation from the beginning to the completion, which shows that our strategy is efficient.

We show a visual comparison of the detection results of our proposed MVODM with Faster R-CNN in Figure 12. The first and second rows show the detection success cases, which include single and multiple targets, large and small scales, and different battlefield environments. From these two rows, we can see that our MVODM has excellent detection performance and is able to locate and detect the target better. While

TABLE 2. Comparison of the detection effectiveness of our MVODM with several other mainstream object detection algorithms. T: Tank, RA: Rocket artillery, IFV: Infantry fighting vehicles, MT: Military trucks, MCV: Military command vehicle vehicle.

Test Subsets	Methods	AP(%)					mAP(%)
		T	RA	IFV	MT	MCV	
L	R-FCN	83.5	80.8	72.4	74.8	71.8	76.7
	SSD	82.8	79.6	72.6	74.3	71.3	76.1
	YOLOv3	82.7	78.4	70.6	73.6	69.4	74.9
	YOLOv4	89.3	90.6	83.5	79.6	75.6	83.7
	Faster R-CNN	85.3	81.7	74.7	76.5	72.8	78.2
	MVODM(Ours)	91.8	89.4	82.3	84.6	80.1	85.6
S	R-FCN	66.3	60.6	54.2	59.2	51.3	58.3
	SSD	64.7	59.3	53.8	57.3	50.7	57.2
	YOLOv3	59.6	58.4	51.6	55.4	49.3	54.9
	YOLOv4	67.4	68.5	56.1	58.9	54.8	61.1
	Faster R-CNN	65.1	61.2	54.4	58.1	52.2	58.2
	MVODM(Ours)	73.4	70.4	61.7	65.3	60.6	66.3
A	R-FCN	78.5	72.8	66.3	67.9	62.7	69.6
	SSD	76.4	72.3	65.7	67.2	62.4	68.8
	YOLOv3	75.8	71.1	62.4	65.3	60.4	67.0
	YOLOv4	82.3	76.8	69.5	71.6	67.8	73.6
	Faster R-CNN	79.8	74.4	67.2	70.1	64.3	71.2
	MVODM(Ours)	86.7	83.2	78.4	80.9	76.5	81.1

Faster R-CNN is able to detect some of the targets, there is a missed detection on smaller scale targets, such as the tank in the fourth column of the first row. Also false detection occurs on confusable targets, such as the infantry fighting vehicle in the second row and third column is mistakenly detected as a tank. Moreover, the localization box of Faster R-CNN is rougher compared to our MVODM. The third and fourth rows show some of the failures that occur in the detection, which mainly originate from occlusion (first column) and interference from the environment (second column). Such failures are also present and occur more frequently in the Faster R-CNN. This also reveals that solving the problems of occlusion and environmental interference is the key to further improve the performance of the detector, and is the focus of future research work.

VI. CONCLUSION

Military vehicle object detection technology in complex environments is of great value to information and intelligent warfare. For the problem that the performance of traditional detection algorithms cannot meet the demand of military vehicle detection in complex battlefield environments, this paper proposes an improved detection algorithm MVODM. First, to address the lack of military vehicle target datasets, we construct a reliable dataset MVD by collecting images and videos from the Internet. The MVD contains multi-scale military vehicle targets in multiple operational environments and can help detect models for better training. Then, we propose two improved strategies: a hierarchical feature representation strategy and a reinforcement learning-based refinement localization strategy. The combination of these two strategies can help the detector to get the best refined localization boxes and thus improve the detection performance. In particular, we note that our scheme has good results in solving the multi-scale problem that exists in object detection. Finally, experimental results on homemade dataset show that our proposed MVODM has excellent detection performance and is able to perform the detection task of military vehicles well.

REFERENCES

[1] A. Miller, "Situational awareness-from the battlefield to the corporation," *Comput. Fraud Secur.*, vol. 2006, no. 9, pp. 13–16, Sep. 2006.

[2] H. Peng, Y. Zhang, S. Yang, and B. Song, "Battlefield image situational awareness application based on deep learning," *IEEE Intell. Syst.*, vol. 35, no. 1, pp. 36–43, Jan. 2020, doi: 10.1109/MIS.2019.2953685.

[3] O. Nave and M. Elbaz, "Artificial immune system features added to breast cancer clinical data for machine learning (ML) applications," *Biosystems*, vol. 202, Apr. 2021, Art. no. 104341.

[4] Y. Ren, A. Liu, X. Mao, and F. Li, "An intelligent charging scheme maximizing the utility for rechargeable network in smart city," *Pervas. Mobile Comput.*, vol. 77, Oct. 2021, Art. no. 101457.

[5] G. Matthews, P. A. Hancock, J. Lin, A. R. Panganiban, L. E. Reinerman-Jones, J. L. Szalma, and R. W. Wohleber, "Evolution and revolution: Personality research for the coming world of robots, artificial intelligence, and autonomous systems," *Personality Individual Differences*, vol. 169, Feb. 2021, Art. no. 109969, doi: 10.1016/j.paid.2020.109969.

[6] V. Neagoe, S. Carata, and A.-D. Ciotec, "An advanced neural network-based approach for military ground vehicle recognition in SAR aerial imagery," *Sci. Res. Educ. Air Force*, vol. 18, pp. 41–48, Jun. 2016.

[7] M. Chen, W. Liu, T. Wang, S. Zhang, and A. Liu, "A game-based deep reinforcement learning approach for energy-efficient computation in MEC systems," *Knowl.-Based Syst.*, vol. 235, Nov. 2022, Art. no. 107660.

[8] M. Chen, A. Liu, W. Liu, K. Ota, M. Dong, and N. N. Xiong, "RDRL: A recurrent deep reinforcement learning scheme for dynamic spectrum access in reconfigurable wireless networks," *IEEE Trans. Netw. Sci. Eng.*, vol. 9, no. 2, pp. 364–376, Mar. 2022, doi: 10.1109/TNSE.2021.3117565.

[9] N. Dalal and B. Triggs, "Histograms of oriented gradients for human detection," in *Proc. IEEE Comput. Soc. Conf. Comput. Vis. Pattern Recognit.*, vol. 1, no. 1, Jun. 2005, pp. 886–893, doi: 10.1109/CVPR.2005.177.

[10] P. Viola, M. J. Jones, and D. Snow, "Detecting pedestrians using patterns of motion and appearance," *Int. J. Comput. Vis.*, vol. 63, no. 2, pp. 153–161, 2005.

[11] S. Walk, N. Majer, K. Schindler, and B. Schiele, "New features and insights for pedestrian detection," in *Proc. IEEE Comput. Soc. Conf. Comput. Vis. Pattern Recognit.*, Jun. 2010, pp. 1030–1037, doi: 10.1109/CVPR.2010.5540102.

[12] T. Ojala, M. Pietikäinen, and D. Harwood, "A comparative study of texture measures with classification based on featured distributions," *Pattern Recognit.*, vol. 29, no. 1, pp. 51–59, 1996.
[13] P. Dollár, Z. Tu, P. Perona, and S. Belongie, *Integral Channel Features*. Birmingham, U.K.: BMVA Press, Sep. 2009, pp. 91.1–91.11, doi: 10.5244/C.23.91.
[14] K. Simonyan and A. Zisserman, "Very deep convolutional networks for large-scale image recognition," 2014, *arXiv:1409.1556*.
[15] A. Krizhevsky, I. Sutskever, and G. E. Hinton, "ImageNet classification with deep convolutional neural networks," *Commun. ACM*, vol. 60, no. 2, pp. 84–90, Jun. 2012.
[16] R. Girshick, J. Donahue, T. Darrell, and J. Malik, "Rich feature hierarchies for accurate object detection and semantic segmentation," in *Proc. IEEE Conf. Comput. Vis. Pattern Recognit.*, Jun. 2014, pp. 580–587.
[17] R. Girshick, "Fast R-CNN," in *Proc. IEEE Int. Conf. Comput. Vis. (ICCV)*, Dec. 2015, pp. 1440–1448.
[18] S. Ren, K. He, R. Girshick, and J. Sun, "Faster R-CNN: Towards real-time object detection with region proposal networks," in *Proc. Adv. Neural Inf. Process. Syst.*, vol. 28, 2015, pp. 1–9.
[19] J. Redmon, S. Divvala, R. Girshick, and A. Farhadi, "You only look once: Unified, real-time object detection," in *Proc. IEEE Conf. Comput. Vis. Pattern Recognit. (CVPR)*, Jun. 2016, pp. 779–788.
[20] J. Redmon and A. Farhadi, "YOLO9000: Better, faster, stronger," in *Proc. IEEE Conf. Comput. Vis. Pattern Recognit. (CVPR)*, Jul. 2017, pp. 6517–6525.
[21] J. Redmon and A. Farhadi, "YOLOv3: An incremental improvement," 2018, *arXiv:1804.02767*.
[22] A. Bochkovskiy, C.-Y. Wang, and H.-Y. M. Liao, "YOLOv4: Optimal speed and accuracy of object detection," 2020, *arXiv:2004.10934*.
[23] W. Liu, "SSD: Single shot multibox detector," in *Proc. Eur. Conf. Comput. Vis.* Cham, Switzerland: Springer, 2016, pp. 21–37.
[24] S. Hao-Ze, C. Tian-Qing, W. Quan-Dong, K. De-Peng, and D. Wen-Jun, "Image detection method for tank and armored targets based on hierarchical multi-scale convolution feature extraction," *Acta Armamentarii*, vol. 38, no. 9, p. 1681, 2017.
[25] Q. Wang, J. Zhang, X. Hu, and Y. Wang, "Automatic detection and classification of oil tanks in optical satellite images based on convolutional neural network," in *Proc. Int. Conf. Image Signal Process.* Cham, Switzerland: Springer, 2016, pp. 304–313.
[26] X. Hu, P. Zhang, and Y. Xiao, "Military object detection based on optimal Gabor filtering and deep feature pyramid network," in *Proc. Int. Conf. Artif. Intell. Comput. Sci.*, 2019, pp. 524–530.
[27] S. Liu and Z. Liu, "Multi-channel CNN-based object detection for enhanced situation awareness," 2017, *arXiv:1712.00075*.
[28] Z. Yang, W. Yu, P. Liang, H. Guo, L. Xia, F. Zhang, Y. Ma, and J. Ma, "Deep transfer learning for military object recognition under small training set condition," *Neural Comput. Appl.*, vol. 31, no. 10, pp. 6469–6478, 2019.
[29] B. Janakiramaiah, G. Kalyani, A. Karuna, L. Prasad, and M. Krishna, "Military object detection in defense using multi-level capsule networks," *Soft Comput.*, pp. 1–15, Jun. 2021, doi: 10.1007/s00500-021-05912-0.
[30] P. Gupta, B. Pareek, G. Singal, and D. V. Rao, "Edge device based military vehicle detection and classification from UAV," *Multimedia Tools Appl.*, vol. 81, no. 14, pp. 19813–19834, 2022.
[31] T.-Y. Lin, M. Maire, S. Belongie, J. Hays, P. Perona, D. Ramanan, P. Dollár, and C. L. Zitnick, "Microsoft coco: Common objects in context," in *Proc. Eur. Conf. Comput. Vis.* Cham, Switzerland: Springer, 2014, pp. 740–755.
[32] A. Geiger, P. Lenz, and R. Urtasun, "Are we ready for autonomous driving? the KITTI vision benchmark suite," in *Proc. IEEE Conf. Comput. Vis. pattern Recognit.*, Jun. 2012, pp. 3354–3361.
[33] X. Zhang, L. Cheng, B. Li, and H.-M. Hu, "Too far to see? Not really!—Pedestrian detection with scale-aware localization policy," *IEEE Trans. Image Process.*, vol. 27, no. 8, pp. 3703–3715, Mar. 2018.
[34] V. Mnih, N. Heess, and A. Graves, "Recurrent models of visual attention," in *Proc. Adv. Neural Inf. Process. Syst.*, vol. 27, 2014, pp. 2204–2212.
[35] R. S. Sutton and A. G. Barto, *Reinforcement Learning: An Introduction*. Cambridge, MA, USA: MIT Press, 2018.
[36] J. C. Caicedo and S. Lazebnik, "Active object localization with deep reinforcement learning," in *Proc. IEEE Int. Conf. Comput. Vis. (ICCV)*, Dec. 2015, pp. 2488–2496.
[37] J. Deng, W. Dong, R. Socher, L.-J. Li, K. Li, and L. Fei-Fei, "ImageNet: A large-scale hierarchical image database," in *Proc. IEEE Conf. Comput. Vis. Pattern Recognit.*, Jun. 2009, pp. 248–255.
[38] D. P. Kingma and J. Ba, "Adam: A method for stochastic optimization," 2014, *arXiv:1412.6980*.
[39] J. Dai, Y. Li, K. He, and J. Sun, "R-FCN: Object detection via region-based fully convolutional networks," in *Proc. Adv. Neural Inf. Process. Syst.*, vol. 29, 2016, pp. 379–387.

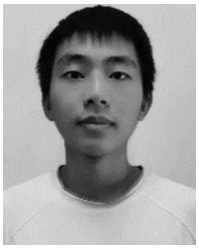

YAN OUYANG was born in Hengyang, Hunan, China, in 1998. He is currently pursuing the master's degree in mechanical engineering with Army Engineering University. His research interests include deep learning, reinforcement learning, and computer vision.

XINQING WANG received the doctor degree. He is currently a Professor and a Doctoral Tutor with Army Engineering University, China. His main research interests include electromechanical control, intelligent signal processing, and computer vision.

RUIZHE HU was born in Xiangyang, Hubei, China, in 1999. He is currently pursuing the master's degree in mechanical engineering with Army Engineering University. His research interests include deep learning, adversarial examples, and object detection.

HONGHUI XU was born in Shantou, Guangdong, China, in 1995. He is currently pursuing the master's degree in mechanical engineering with the College of Field Engineering, Army Engineering University. His research interests include machine learning and computer vision, especially object detection.

FAMING SHAO was born in 1978. He is an Associate Professor with Army Engineering University, China. His research interests include signal processing, deep learning, and software engineering.